Magazine of Civil Engineering

ISSN 2712-8172

journal homepage: http://engstroy.spbstu.ru/

Research article

UDC 699.86

DOI: 10.34910/MCE.114.12

The influence of the sky radiative temperature on the building energy performance

S.V. Korniyenko

Volgograd State Technical University, Volgograd, Russia

✉ *svkorn2009@yandex.ru*

Keywords: building, building energy performance, sky radiative temperature, sky emissivity, clear sky model, cloudy sky model, ambient air, solar radiation, environment.

Abstract. Most of the current sky models correlate with local climatic conditions and specific sites, while not covering different humidity-climatic conditions. In this work, sky emissivity and sky temperature models were reviewed, taking into account the common classification that includes simplified and detailed correlations. The clear-sky and cloudy-sky temperature models were also investigated in detail, employing them for different humidity-climatic conditions (wet, normal and dry) and evaluating their influence on building energy needs. Under clear-sky conditions in winter, the maximum difference between the ambient air temperature and sky temperature is 19 K regardless of humidity-climatic conditions. Under cloudy-sky conditions, it is possible to notice dissimilarities, ranging from 5 K (wet and normal conditions) to 10 K (dry conditions). In summer, under clear-sky conditions, the maximum values are ranging from 12 K (normal conditions) to 13 K (wet and dry conditions). Under cloudy-sky conditions, the maximum values are ranging from 5 K (normal conditions) to 10 K (dry conditions). Thus, the obtained results can be applied for the investigation of the radiative heat flux between a building surface and the sky, as a simplified model. Moreover, these results can be used when the sky temperature is not available from climatic data. The obtained results specified the simplified models according to ISO 13790. Finally, taking into account the influence of different correlations in building energy simulations, it was found that heating and cooling energy demands (using the example of a translucent roof) can be affected by significant percentage differences (the rounded values), ranging from +3 % to +11 % (no heat gain) for wet climatic conditions, from –61 % to +22 % for normal climatic conditions, and, finally, from −45 % to +8 % for dry climatic conditions. The comparison among the models can be useful to address the choice of users in building energy simulations and engineering applications. Future developments will regard the longwave sky radiation measurement under field conditions in the representative cities of the world in order to propose correlations for different climatic area.

Citation: Korniyenko, S.V. The influence of the sky radiative temperature on the building energy performance. Magazine of Civil Engineering. 2022. 114(6). Article No. 11412. DOI: 10.34910/MCE.114.12

1. Introduction

Heat transfer between the exterior surface of a building and the environment is based on convective and radiative phenomena [1]. This process included shortwave radiation, including direct, reflected and diffuse sunlight, longwave radiation to the environment, convective exchange with outside air [2, 3]. Thermal exchange associated to the sky longwave radiation can be related to an effective sky temperature [4]. Nowadays, building energy simulations use models able to estimate the temperature of the sky [3]. The sky can be thought as a heat sink for the exterior surfaces and the sky longwave radiation exchange is a function of the effective sky temperature [5–7]. The radiative cooling is highest during the night when the sky is clear, and humidity is low [8, 9]. In winter, the radiative cooling is negative factor as the temperature decrease on the exterior surface of a building increases heat loss [10]. In summer radiative passive cooling

is positive factor which employs thermal radiation properties for cooling an object or part of a building facing a colder surface, such as the sky [11–13]. The building sector covers about 40 % of total energy consumption [14–16]. Every second resident of the Earth lives in the city [17]. Buildings energy demand is increasing in connection with the growth of cities [18–23].

In order to evaluate radiative heat exchanges between a building and environment, sky emissivity and sky temperature needs to be assessed.

The first study related to the sky emissivity prediction was performed by Angström [24]. His model was developed starting from a long series of observations conducted in Algeria. The Angström's model is a function of the actual atmospheric vapor pressure. Many researchers developed their models starting from the Angstrom's correlation, modifying it with adapted coefficients.

Brunt [25] proposed a sky emissivity formula based on the correlation between sky temperature and the partial pressure of water vapor. This formula gives the sky emittance as a linear function of the square root of water vapor partial pressure. The equation needs the calculation of empirical coefficients, variable in function of the analyzed geographical region.

Clark and Allen [26] proposed formula for different meteorological conditions. This formula gives the clear sky emittance as a linear function of the natural logarithm of dew point.

Idso [27] proposed his correlation based on measurements conducted in Arizona (USA). His correlation can be employed for the whole range of wavelength, accounting water vapor pressure and ambient temperature.

Berdahl and Martin [27, 28] collected a set of almost 5 years sky longwave radiation data in 6 different cities. The model can be used for dew point temperatures which range between −13 °C and +24 °C.

Many others studies have been conducted on sky emissivity and sky temperature models and different correlations have been proposed by researchers [26, 27, 29, 30, 31, 32] (authors E.L. Andreas, S.F. Ackley, C.V. Melchor, J.L. Hatfield, R.J. Reginato, B. Chen, D. Clark, J. Maloney, W. Mei, J. Kasher and W. Swinbank, et al). The paper [27] (authors L. Evangelisti, C. Guattari, F. Asdrubali) gives a critical review about the existing correlations for the calculation of sky emissivity and sky temperature, referring to different climatic conditions.

Sky models are related to local meteorological conditions and specific sites [33]. Most of these models are approximated due to the lack of detailed measured data. The aim of this paper is providing a comparative analysis of different model of the sky as the clear sky and cloudy sky, also the calculation of the sky emissivity and sky temperature, relating them to the different humidity conditions in Russia. The correlations were used to quantify similarities and differences among them. The effect of different correlations on heating and cooling energy demands was examined.

2. Methods

2.1. Sky emissivity and sky temperature models

The radiation related to the atmosphere can be expressed assuming that the sky has the same behavior of a black body (characterized by an emissivity equal to 1) or assuming that the sky is a grey body, distinguished by an apparent emissivity [32, 34]. According to this, two relations can be identified:

$$q_{sky} = \sigma T_{sky}^4, \tag{1}$$

$$q_{sky} = \varepsilon_{sky} \sigma T_{amb}^4, \tag{2}$$

where q_{sky} is the atmospheric radiation, σ is the Stefan-Boltzmann constant (σ = 5.67·10^{-8} W·m^{-2}·K^{-4}), T_{sky} is the sky radiative temperature (sky temperature), ε_{sky} is the emissivity of the sky and T_{amb} is the ambient temperature (temperatures T_{sky} and T_{amb} are in degrees Kelvin). Making equal Eqs. (1) and (2), it is possible to obtain:

$$T_{sky} = \sqrt[4]{\varepsilon_{sky}} T_{amb}. \tag{3}$$

The net radiative heat flux $\left(q_{rad}\right)$ between a building surface and the sky can be quantified as follows [27, 34]:

$$q_{rad} = \varepsilon\sigma F\left(T_s^4 - T_{sky}^4\right), \quad (4)$$

where ε is the hemispherical emissivity of the surface, F is the sky view factor and T_s is the surface temperature.

T_{sky} can be defined as an equivalent temperature of the sky vault. It is worthy to notice that the sky temperature is an average over the sky dome. The coldest part of the sky is the dome overhead. At the horizon, the temperature of the sky is equal to the ambient temperature. Subsequently, the usual approximation of considering a sky view factor equal to 0.5 for vertical surfaces (implicitly assuming a uniform sky temperature) can be considered an approximation adopted in simulation codes to simplify calculations but it cannot be considered fully representative [10].

The mentioned equations make easier the estimation of the inward infrared radiation from the atmosphere. Nevertheless, this is not generally measured by weather stations. Therefore, correlations have been developed in order to relate the climatic parameters to the infrared atmospheric radiation.

It is worthy to notice that sky temperature and ambient temperature are different. Starting from ground and going upward, temperatures tend to decrease, with a resulting sky temperature lower than the air temperature [25]. Furthermore, the difference between sky and air temperatures is higher during the summer, especially when clear sky conditions occur. Moreover, the effective sky temperature depends on other many factors, such as dew point, clouds amount and the site conditions. Therefore, these factors need to be considered during the study and development of sky temperature models.

Several correlations are nowadays available to calculate the clear-sky emissivity and temperature of the sky [27], coming from different methods for the infrared radiation estimation. Table 1 lists the four main correlations for the sky emissivity under clear-sky conditions, are widely applicable in the sky radiation modeling.

Table 1. Empirical clear sky models based on emissivity correlations

Author	Correlation
Clark and Allen	$\varepsilon_{sky,clear} = 0.787 + 0.764 \cdot \ln(T_{dp} / 273)$
Martin and Berdahl	$\varepsilon_{sky,clear} = 0.758 + 0.521(T_{dp} / 100) + 0.625(T_{dp} / 273)^2$
Brunt	$\varepsilon_{sky,clear} = 0.618 + 0.056(P_{wv})^{0.5}$
Idso	$\varepsilon_{sky,clear} = 0.685 + 3.2 \times 10^{-5}(P_{wv}) \exp(1699 / T_{db})$

In Table 1: $\varepsilon_{sky,clear}$ is the clear sky emissivity, is the dew point temperature, in K for Clark and Allen, in °C for Martin and Berdahl, P_{wv} is the partial pressure of water vapor, in hPa, T_{db} is the drybulb temperature, in $K\left(T_{db} \approx T_{amb}\right)$.

It is well-known that clear sky conditions are not continuous along time and cloudy conditions increase the infrared radiation. For this reason, the clear sky correlations have to be adapted to cloudy conditions. The impact of cloudiness on sky temperature is difficult to evaluate, and only a few researchers have attempted to predict it. Berdahl and Martin developed a cloudy emissivity model based on a cloudiness factor $\left(CF\right)$. This factor ranges between 0 and 1, depending on clear sky conditions or totally cloudy sky. Thus, the sky temperature modeling is based on the following equation [27]:

$$T_{sky} = T_{amb}\left[\varepsilon_{sky,clear} + 0.8\left(1 - \varepsilon_{sky}\right)CF\right]^{0.25}. \quad (5)$$

It is worthy to notice that, in the above formula, a factor equal to 0.8 appears. The reason of this value (instead of 1) is related to a cloud base temperature significantly lower than the air temperature at screen height.

If weather data do not contain the sky cloudiness factor, it can be determined according to the Kasten and Czeplak formula [6]:

$$CF = \left(1.4286\frac{G_{dif}}{G_{Glob,H}} - 0.3\right)^{0.5}, \quad (6)$$

where G_{dif} is the diffuse radiation on the horizontal and $G_{Glob,H}$ is the total radiation on the horizontal. CF can be used to calculate the effective sky temperature by means of Eq. (3).

Nowadays, simplified methods for calculating the sky temperature are well-known.

Taking into account the heat transfers between buildings and the environment, if data for the sky temperature calculation are not available, ISO 13790 allows to calculate the temperature of the sky, considering the equations listed in Table 2. The standard provides a simplified calculation method for determining the annual energy requirement for heating in residential and non-residential buildings. Starting from the building location, it is possible to define the climatic area and consequently identify the suitable correlation. It is possible to distinguish different climatic areas, according to the common world climate classification proposed by Köppen [35]. It is worthy to notice that ISO 13790 takes into account a climate classification based only on latitudes, distinguishing sub-polar, temperate and tropical areas. The classification of humidity areas in Russia is proposed by Ilyinsky for simplified calculations according to SP 50.13330.2012 (National Standard). According to this classification, wet, normal and dry zones are distinguished.

Table 2. Simplified models according to ISO 13790.

Site	Correlation
Temperate areas	$T_{sky} = T_{amb} - 11$
Sub-polar areas	$T_{sky} = T_{amb} - 9$
Tropical areas	$T_{sky} = T_{amb} - 13$

Calculations using simplified models according to ISO 13790 are not always representative for temperate areas with humidity variations.

According to SP 50.13330.2012 (National Standard) the sky emissivity is equal to 1, and the sky temperature is equal to the ambient temperature. Obviously, this simplified model cannot ensure the representativeness and accuracy of the calculation results.

2.2. Outside surface heat balance

The different sky temperature models can be used to model a building energy performance. The heat balance on the outside face of building element is:

$$q_{asol} + q_{LWR} + q_{conv} - q_{cond} = 0, \quad (7)$$

where q_{asol} is the absorbed direct and diffuse solar (short wavelength) radiation heat flux, q_{LWR} is net long wavelength (thermal) radiation flux exchange with the air and surroundings, q_{conv} is convective flux exchange with outside air and q_{cond} is conduction heat flux into the building elopement (heat fluxes q_{asol}, q_{LWR}, q_{conv}, and q_{cond} are in W/m^2). Simplified procedures generally combine the first three terms by using the concept of a sol-air temperature [36].

Generally, the exterior surface heat flux $\left(q_{se}\right)$ is given by equation:

$$q_{se} = -pG_{Glob} + h_{ce}\left(T_{se} - T_{out}\right) + h_{re}\left(T_{se} - T_{sky}\right), \quad (8)$$

were p is the solar absorptance coefficient, G_{Glob} is the total radiation on the surface, h_{ce} is the surface exterior convective heat transfer coefficient, T_{out} is the outdoor air temperature, h_{re} is the surface exterior radiative heat transfer coefficient and T_{sky} is the clear or cloudy sky temperature. A venerable equation for wind-driven convection was developed by W.H. McAdams (1954) which Palyvos (2008) casts in SI units as:

$$h_{ce} = 5.7 + 3.8V_z, \quad (9)$$

where V_z is the wind velocity that has been adjusted for height above ground using the z axis coordinate of the surface's centroid. This model can be applied to all surfaces and the relatively large constant is assumed to represent the natural convection portion of a total convection coefficient. The model is not sensitive to wind direction or surface roughness.

The surface radiative heat transfer coefficient can be approximately calculated according to formula ISO 6946:2017:

$$h_{re} = 4\sigma F \varepsilon T_{mn}^3, \quad (10)$$

where T_{mn} is the main thermodynamic temperature of the surface and its surroundings. Taking into account external surfaces, the long-wave radiation transfer at the external surface is accounted employing a sky temperature $\left(T_{sky}\right)$ and a sky view factor $\left(F_{sky}\right)$. For vertical walls and isolated buildings, a realistic value for F_{sky} is 0.5. If there are constructions or trees in front of the wall, the value of F_{sky} should be lower than 0.5. For horizontal surfaces F_{sky} is equal to 1.

The heat flux through the building element $\left(q_{cond}\right)$ is given by well-known equation, so is not discussed in this paper.

3. Results and Discussion

3.1. Models comparison

Starting from the available empirical correlations, some of them were employed to calculate and compare sky emissivity and sky temperatures, employing the Typical Meteorological Years (TMY) [4] available for different cities, in particular considering locations characterized by different humidity-climatic conditions. The averaging period of climatic data of 10 years was considered according to ISO 13788:2012. Wet, normal and dry conditions were considered according to SP 131.13330.2018 (National Standard). According to this, three representative cities were selected (see Table 3).

Table 3. Cities, humidity-climatic zones and correlations tested under clear sky and cloudy sky conditions.

Correlation	City	Humidity-climatic conditions
Clark and Allen	St. Petersburg	Wet
Martin and Berdahl	Moscow	Normal
Brunt	Volgograd	Dry
Idso		

The average climatic data for each city (air temperature, humidity, cloudiness, wind speed) are calculated for the period of 10 years (from 2011 to 2020), using hourly or three-hour values. Different correlations were applied, considering clear and cloudy sky conditions. The comparison among the correlations was achieved taking into account two representative days of January and July.

The climate data calculated using averaging period of 10 years is given in Table 4. Analyzing obtained values, it is possible to identify that the mean values of climate data in whole are representative.

Table 4. Weather-data calculated using averaging period of 10 years.

	St. Petersburg		Moscow		Volgograd	
	January	July	January	July	January	July
Air temperature, °C	–5.0	17.1	–4.1	20.1	–5.4	24.3
Humidity, %	89	70	86	73	89	51
Cloudiness	0.89	0.52	0.92	0.69	0.55	0.30
Wind speed, m/s	4.1	3.6	1.2	1.7	5.9	4.0

Wet conditions. Analyzing wet conditions, the city of St. Petersburg was selected. Summer is short and wet; winter is long, cold and raw. The rainfall average value is equal to 662 mm per year. The average

annual temperature is equal to 5.8 °C. The lowest average temperatures during the year occur in January (minus 5.5 °C). July is the warmest month, characterized by an average temperature of 18.8 °C.

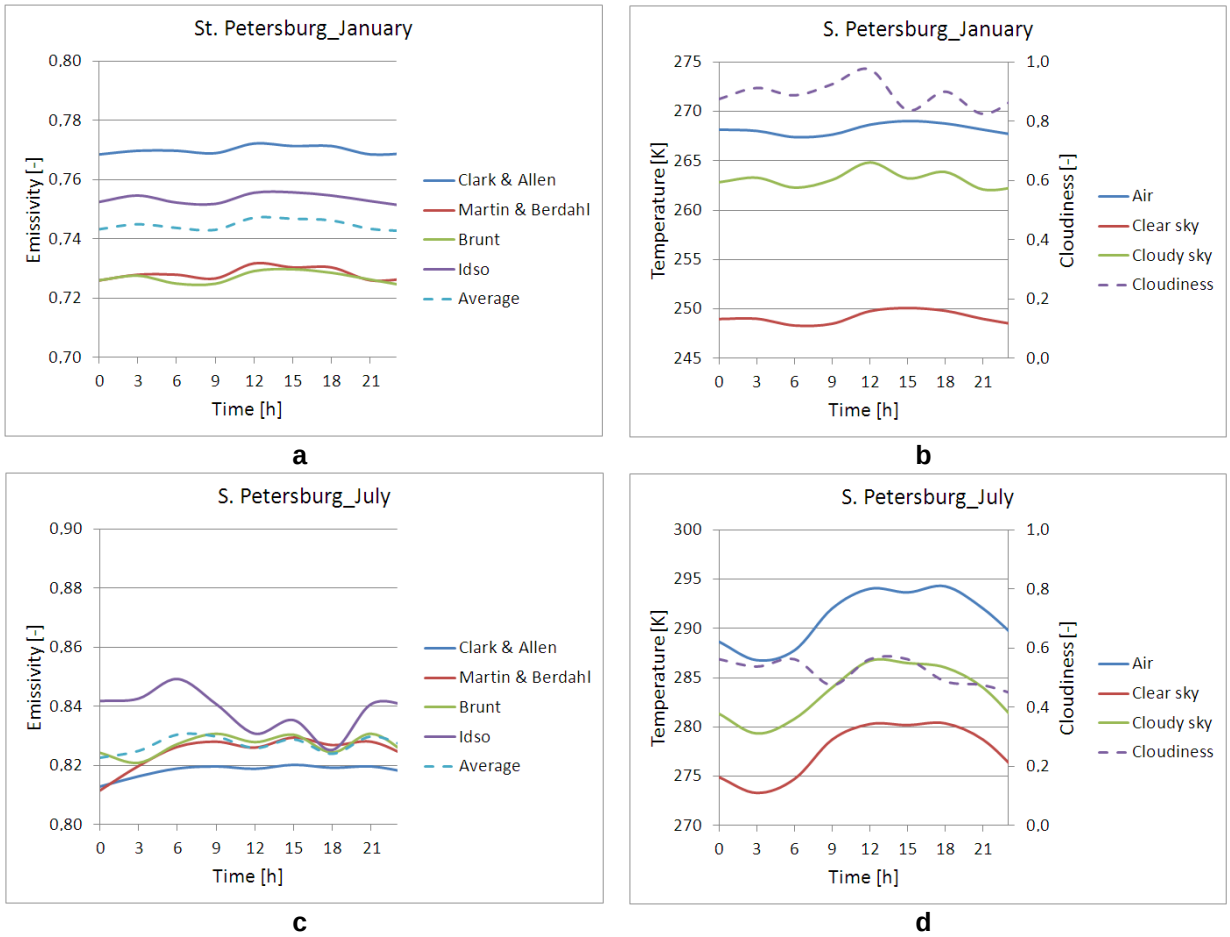

Figure 1. Comparison among the emissivity and sky temperatures calculated using different models in St. Petersburg, during January (a, b) and July (c, d).

Fig. 1 shows the emissivity and the sky temperatures obtained in January and July. In addition, Fig. 1b and d show cloudiness. Both in terms of emissivity and sky temperatures, it is possible to observe a wide variety of values. In winter, Clarc and Allen formula provides the highest emissivity value (with a mean value equal to 0.77), followed by the almost constant trends provided by Idso (mean value equal to 0.73), Martin and Berdahl (mean value equal to 0.73) and Brunt (mean value equal to 0.73). Moreover, it is possible to observe that the Brunt's model allows to calculate emissivity values close to those achieved by means of Martin and Berdahl formula. The emissivity values calculated through the formulae are the lowest. In summer, it is possible to notice the same distribution among the sky emissivity correlations, with the highest values obtained from Idso's formula and the lowest obtained from Clarc and Allen equation. In this case, Brunt's formula provides emissivity values very close to those obtained by means of Martin and Berdahl equation. The emissivity and cloudiness have an influence on sky temperature values, both in winter and in summer. The sky temperature only approximate to ambient air temperature in the case of very cloudy conditions. Analyzing Fig. 1, it is possible to identify that the mean values of emissivity and the sky temperature are fully representative.

Normal conditions. Moscow was selected to analyze the normal climatic condition. The climate of Moscow is moderately continental, with clear seasonality. The average annual temperature is equal to 5.8 °C. January is the coldest month, characterized by an average temperature of minus 6.5 °C. July is the warmest month (with average temperature of 19.2 °C).

Fig. 2 shows the emissivity and the sky temperatures obtained for a representative day of January and July. In January (Fig. 2a), it is possible to observe low emissivity values related to low ambient temperatures. The highest average value can be obtained applying the Clarc and Allen correlation (ε_{avg} = 0.77). On the contrary, the lowest one is obtained with the Martin and Berdahl as well as equation Brunt equations (ε_{avg} = 0.73). During the day the emissivity are quite constant and, subsequently also the sky temperatures are constant (see Fig. 2b). The lowest sky temperatures can be obtained applying the

clear sky model. The highest sky temperatures can be obtained applying the fully cloudiness sky model. All the other correlations provide sky temperature values between these two limit values. On the other hand, in July emissivity and sky temperatures (see Fig. 2c, d) are more variables than in January. In this case, the highest emissivity values are obtained using Idso's correlation. On the contrary, the lowest emissivity values can be obtained applying the Clarc and Allen equation.

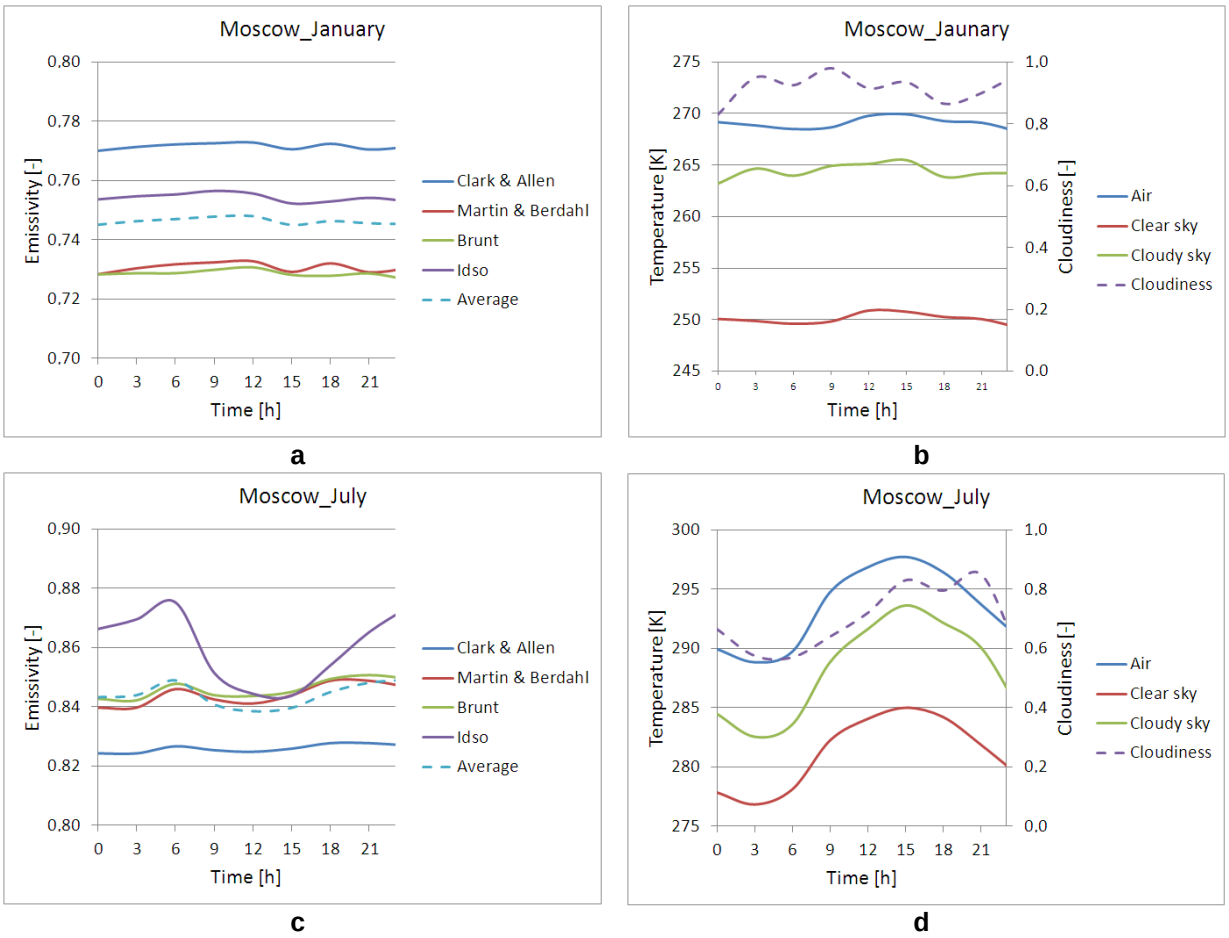

Figure 2. Comparison among the emissivity and sky temperatures calculated using different models in Moscow, during January (a, b) and July (c, d).

Dry conditions. Considering dry conditions, Volgograd (until 1961 – Stalingrad) was selected. The climate is continental. The average rainfall is 267 mm per year. Winter is mild, with frequent thaws, summer is hot and long, at all times of the year sharp temperature variations are possible. The average annual temperature is 8.8 °C. January is the coldest month of the year, with an average temperature of minus 5.7 °C. July is the hottest month of the year, with an average temperature of 24.2 °C. Temperatures during the whole year are characterized by variations approximately equal to 15 °C, on average. The highest total (direct and diffuse) radiation on the horizontal surface in July is 866 W/m^2.

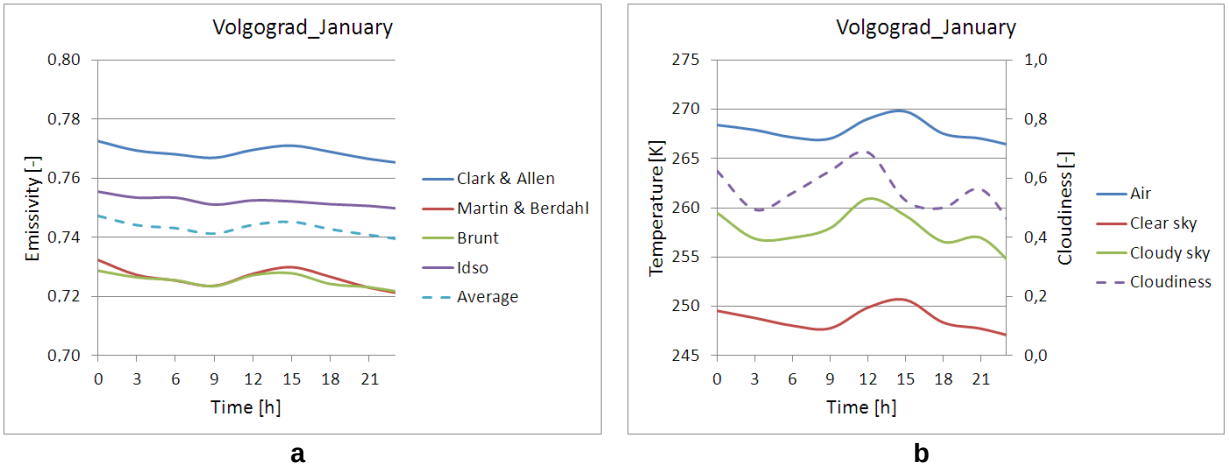

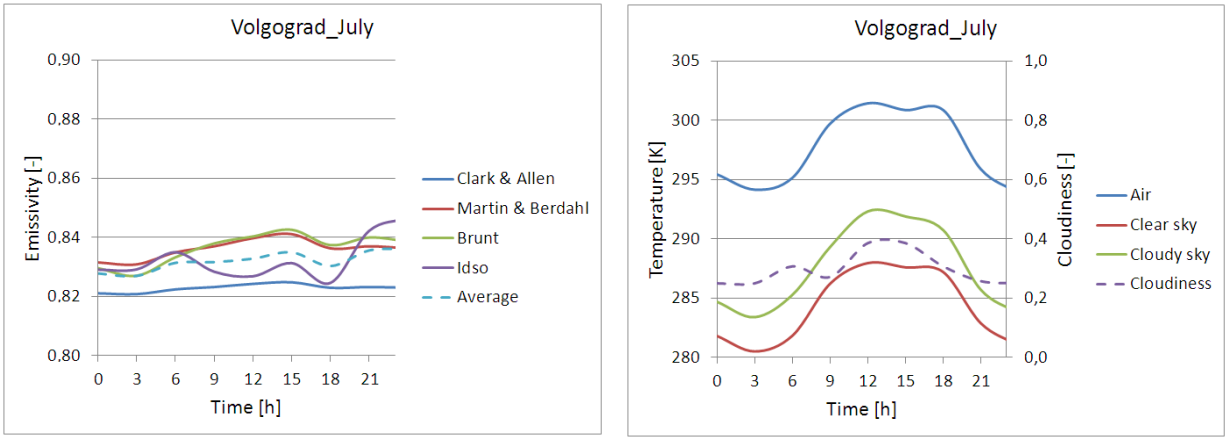

c d

Figure 3. Comparison among the emissivity and sky temperatures calculated using different models in Volgograd, during January (a), (b) and July (c), (d).

Fig. 3a and c show the emissivity values obtained by applying the correlations mentioned before. Fig. 3b and d provide sky temperatures, compared to ambient temperatures in January and July. In January, the correlations suggested by Martin and Berdahl and Brunt provide very similar emissivity. On the other hand, Martin and Berdahl correlation is quite higher. Clarc and Allen equation provides the highest emissivity values. Analyzing the sky emissivity in July, similar values can be obtained applying all the correlations. Fig. 3 shows that the sky temperatures are totally characteristic.

In order to make a comparison, all the average sky emissivity and the average sky temperatures calculated for the aforementioned climatic conditions are summarized in Table 5, 6.

Table 5. Average sky emissivity for clear sky conditions.

Month	Correlation	St. Petersburg (Wet)	Moscow (Normal)	Volgograd (Dry)
January	Clark and Allen	0.77	0.77	0.77
	Martin and Berdahl	0.73	0.73	0.73
	Brunt	0.73	0.73	0.73
	Idso	0.75	0.75	0.75
July	Clark and Allen	0.82	0.83	0.82
	Martin and Berdahl	0.82	0.84	0.84
	Brunt	0.83	0.85	0.84
	Idso	0.84	0.86	0.83

Table 6. Average sky emissivity, cloudiness and sky temperatures for clear and cloudy sky conditions.

Site	Clear sky				Cloudy sky			
	January		July		January		July	
	ε_{avg}	$T_{sky,avg}$, K	ε_{avg}	$T_{sky,avg}$, K	CF_{avg}	$T_{sky,\,avg}$, K	CF_{avg}	$T_{sky,\,avg}$, K
St. Petersburg (Wet)	0.74	249	0.83	277	0.89	263	0.52	283
Moscow (Normal)	0.75	250	0.84	281	0.92	264	0.69	288
Volgograd (Dry)	0.74	249	0.83	284	0.55	258	0.30	287

Analyzing the average sky emissivity in January and July, the correlations suggested by Clark and Allen, Martin and Berdahl, Brunt and Idso provide very similar emissivity. The sky emissivity values in July are more than in January. This conclusion is well correspond to results of Evangelisti, Guattari, Asdrubali and other researchers [27]. Moreover, it is possible to observe that emissivity values are almost the same for different humidity areas; therefore, any correlation can be used, distinguishing winter and summer conditions.

Distinguishing winter and summer conditions, it is possible to observe the sky temperature range obtained by applying the different correlations (see Table 7). Under wet conditions, the sky temperature ranges between 249 K and 263 K in winter (for clear and cloudy sky). During summer, it ranges between 277 K and 283 K. Under winter normal conditions, the sky temperature ranges from 250 K to 264 K, and

during summer, it ranges between 281 K and 288 K. Finally, under dry conditions, the range goes from 249 K to 258 K, and during summer, it goes from 284 K to 287 K.

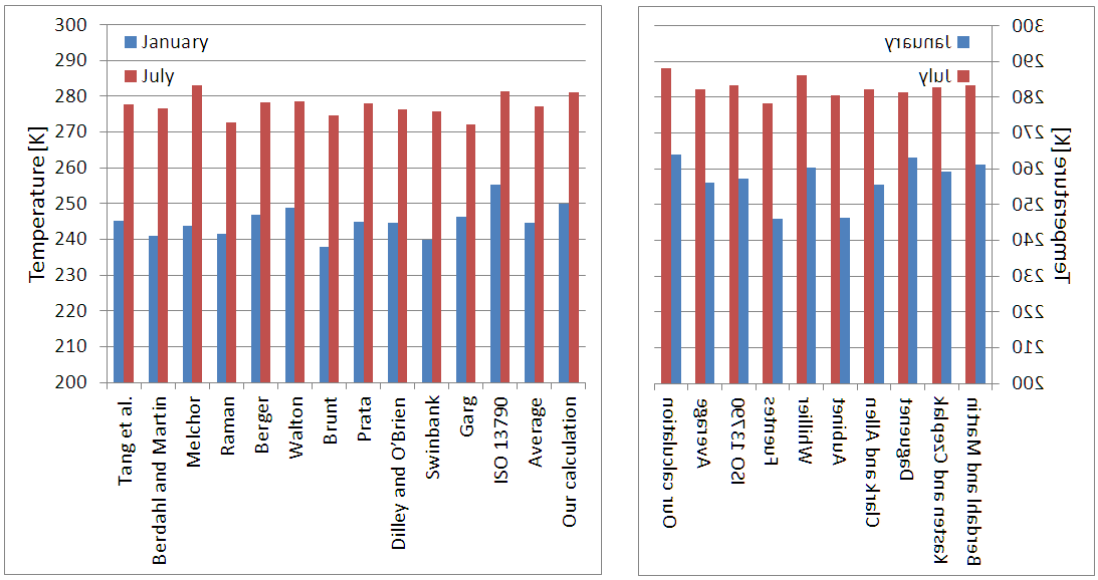

Figure 4. Comparison among the sky temperatures calculated using different models in January (a) and July (b).

Analyzing the obtained data (see Fig. 4) it is worthy to notice that the average sky temperature in whole correlation with results of different study [27]. Percentage differences obtained by using different correlation under clear sky conditions are 2.16 % (in January) and 1.42 % (in June); for cloudy sky conditions – 3.04 % and 2.03 %, respectively.

The obtained results can be applied for specification of the simplified sky temperature models (ISO 13790 and SP 50.13330.2012) taking account the sky model, humidity-climatic conditions and season (see Table 7).

Table 7. Simplified sky temperature model (our suggestions).

Humidity-climatic conditions	Correlation			
	Clear sky		Cloudy sky	
	Winter	Summer	Winter	Summer
Wet	$T_{sky} = T_{amb} - 19$	$T_{sky} = T_{amb} - 13$	$T_{sky} = T_{amb} - 5$	$T_{sky} = T_{amb} - 8$
Normal	$T_{sky} = T_{amb} - 19$	$T_{sky} = T_{amb} - 12$	$T_{sky} = T_{amb} - 5$	$T_{sky} = T_{amb} - 5$
Dry	$T_{sky} = T_{amb} - 19$	$T_{sky} = T_{amb} - 13$	$T_{sky} = T_{amb} - 10$	$T_{sky} = T_{amb} - 10$

Thus, the obtained results can be applied for investigation the radiative heat flux between a building surface and the sky, as simplified model. Also these results can be used when the sky temperature is not available from climatic data.

3.2. Influence of the sky temperature in building energy simulations

The simple isolated building component was modeled considering the typical construction technique of the most recent buildings. The modeling object is a light-transmitting roof. The structure consist some material layers as a “no mass” materials. This assumption essentially says that these layers add nothing to the thermal mass of the overall construction and only add to the overall resistance (R-value) of the construction as a whole. For this reason under passive steady state the heat balance equation for the building element are provided. The thermal resistance of the roof is equal to 1.73 m^2·K/W. The envelope has a solar absorptance coefficient equal to 0.7. Heat losses and heat gains through other building elements is expected to be negligible. The indoor setpoint temperature was set equal to 20 °C for heating and 24 °C for cooling.

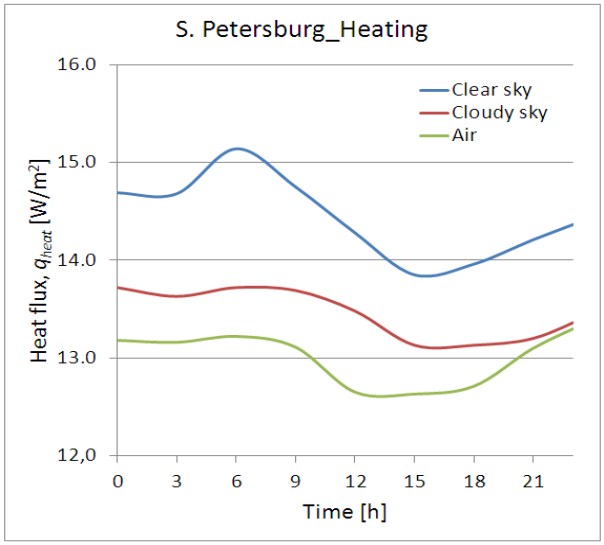

a

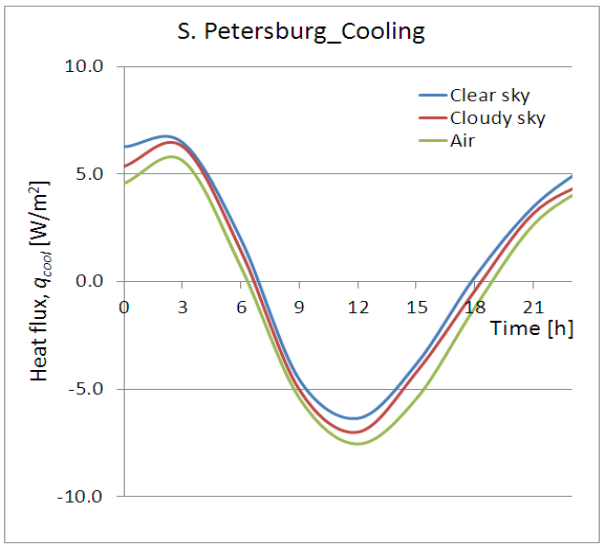

b

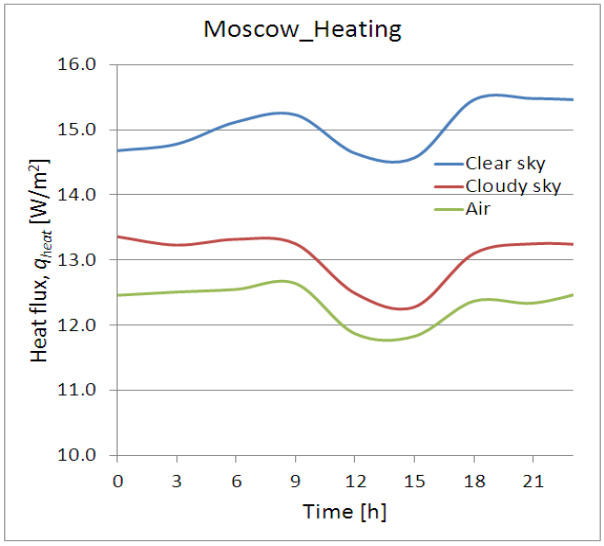

c

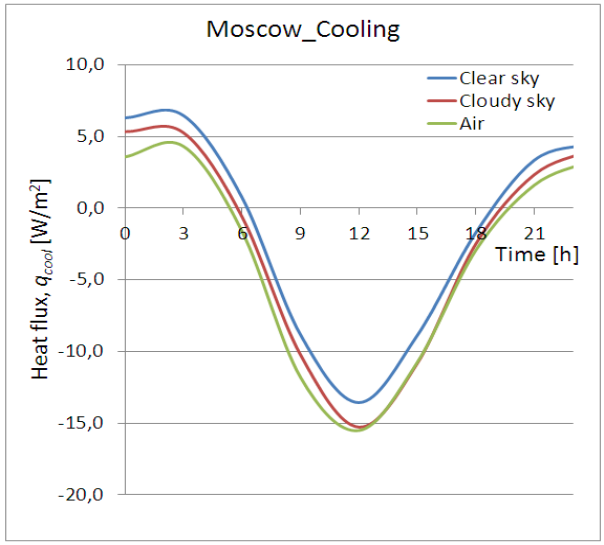

d

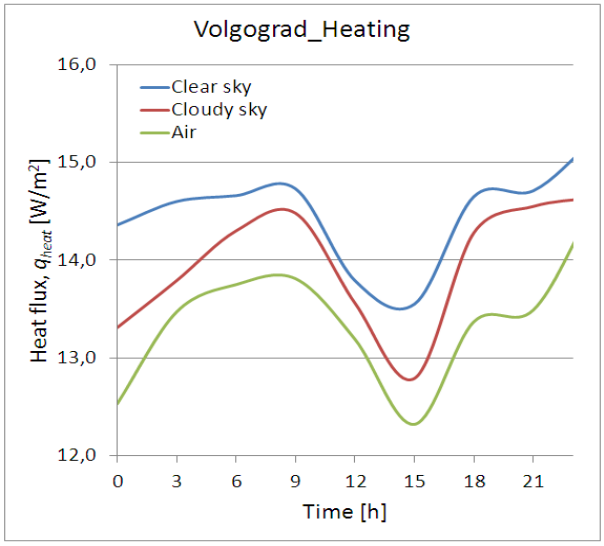

e

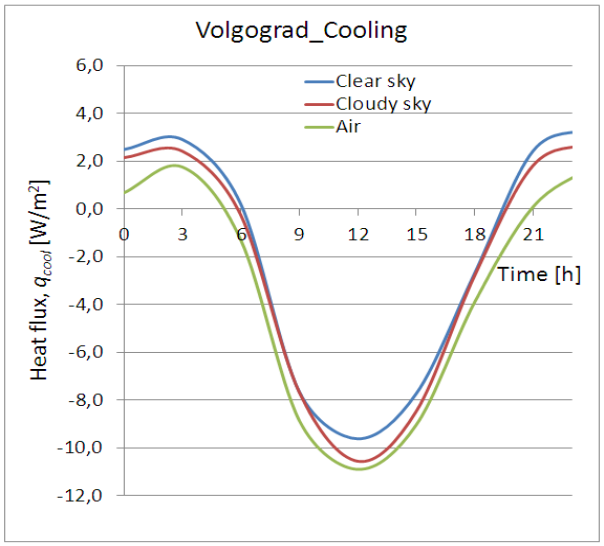

f

Figure 5. Heat flux variations for heating (q_{heat}) and cooling (q_{cool}), using different sky temperature models. St. Petersburg (a, b); Moscow (c, d); Volgograd (e, f).

Starting from this, heating and cooling energy needs were simulated (for coldest and hottest days), and the obtained results are shown in Fig. 5. In this stage, three models were tested (clear sky, cloudy sky and ambient air).

Analyzing the data it is worthy to notice that the heat flux fluctuations through the building component are different in winter and summer. Positive values of the heat flow correspond to heat losses, negative values are the heat gains. In January, the heat flux fluctuations are non-harmonic, which can be explained by the variable effect of the heat and cold waves on the structure. The maximum heat flux values occur during the morning and evening, minimum values – in daytime. In July, the heat flux fluctuations are harmonic, with maximum values at 0–3 a.m. and minimum values at 12 p.m. The heat flux is vary depending on the sky temperature. The highest heat flux value can be obtained applying the clear sky model, the lowest value in the case of ambient temperature.

Table 8 lists the percentage differences obtained comparing heating and cooling daily energy needs. The comparison takes into account the three mentioned humidity-climatic conditions and allows to observe what is reported below.

Table 8. Percentage differences (%) obtained by using different sky temperature models.

Sky temperature models	St. Petersburg		Moscow		Volgograd	
	Heating	Cooling	Heating	Cooling	Heating	Cooling
Clear sky	+10.97	no heat gain	+21.87	–61.01	+8.13	–45.16
Cloudy sky	+3.41	no heat gain	+5.76	–24.75	+4.34	–30.66
Ambient air	0.00	0.00	0.00	0.00	0.00	0.00

Wet conditions: in this case, only heating energy need has to be considered. The highest differences can be obtained by using clear sky model (+11 %). The cloudy sky model allows to obtain the differences energy need is +3.4 %.

Normal conditions: the climatic conditions in Moscow produce high heating energy needs. Use the different sky models allow to obtain percentage differences between +21.9 % and +5.8 %. Analyzing cooling energy demands, the percentage difference values are much higher than the other humidity-climatic conditions (–61 % to –24.8 %) but they refer to almost negligible demands for cooling.

Dry conditions: in this case both heating and cooling energy needs have to be simulated. Considering heating energy demands, the highest differences can be obtained by using clear sky model (+8.1 %). The lowest percentage differences can be achieved using the cloud sky model (+4.3 %). The employment of the cloud sky model represents inter-mediate situation, with percentage differences +4.3 %. Analyzing cooling energy demands, the highest differences can be obtained clear sky model (–45.2 %). If the cloud sky model is applied, the percentage difference equal to –30.7 %.

Thus, the temperature of the sky changes the building energy performance: in winter heat losses increase, in summer heat gains decrease. Taking into account the temperature of the sky in the heat transfer process through the building components makes it possible to more accurately calculate the heating and cooling needs of the buildings.

4. Conclusions

Previously, several sky temperature models and different their correlations have been defined by the researchers. Most of the current sky models are correlated to local climatic conditions and specific sites and they do not cover different humidity-climatic conditions. In this work, sky emissivity and sky temperature models were reviewed, taking into account the common classification that includes simplified and detailed correlations. The clear-sky and cloudy-sky temperature models were also investigated in detail, employing them for different humidity-climatic conditions (wet, normal and dry) and evaluating their influence on building energy needs. In winter, under clear-sky conditions the maximum difference between the ambient air temperature and sky temperature is 19 K regardless of humidity-climatic conditions. Under cloudy-sky conditions it is possible to notice dissimilarities, ranging from 5 K (wet and normal conditions) to 10 K (dry conditions). In summer, under clear-sky conditions, the maximum values are ranging from 12 K (normal conditions) to 13 K (wet and dry conditions). Under cloudy-sky conditions, the maximum values are ranging from 5 K (normal conditions) to 10 K (dry conditions). Thus, the obtained results can be applied for investigation the radiative heat flux between a building surface and the sky, as simplified model. Also these results can be used when the sky temperature is not available from climatic data. The obtained results specified the simplified models according to ISO 13790. Finally, taking into account the influence of different correlations in building energy simulations, it was found that heating and cooling energy demands (using the example of a translucent roof) can be affected by significant percentage differences (the rounded

values), ranging from +3 % to +11 % (no heat gain) for wet climatic conditions, from –61 % to +22 % for normal climatic conditions, and, finally, from −45 % to +8 % for dry climatic conditions. The comparison among the models can be useful to address the choice of users in building energy simulations and engineering applications [20, 22]. Future developments will regard the longwave sky radiation measurement under field conditions in the representative cities of the world in order to propose correlations for different climatic area.

References

1. Sparrow, E.M., Cess, R.D. Radiation heat transfer. 1978. 366. ISBN: 0-89116-923-7
2. Kreith, F., Black, W.Z. Basic heat transfer. 1980. 45 (6). DOI: 10.1201/9780203755570-15
3. Musta, L.G., Zhurov, G.N., Belyaev, V.V. Modeling of a solar radiation flow on an inclined arbitrarily oriented surface. Journal of Physics: Conference Series. 2019. 1333 (3). DOI: 10.1088/1742-6596/1333/3/032054
4. Zhang, Q, Joe, H., Lang, S. Development of typical year weather data for Chinese location. ASHRAE Transactions. 2002. 108 (2). LBNL-51436.
5. Walkenhorst, O., Luther, J., Reinhart, C., Timmer, J. Dynamic annual daylight simulations based on one-hour and one-minute means of irradiance data. Solar Energy. 2002. 72 (5). Pp. 385–395. DOI: 10.1016/S0038-092X(02)00019-1
6. Rommel, M. On the estimation of atmospheric radiation from surface meteorological data. 1996. 56 (4). Pp. 349–359.
7. Skartveit, A., Olseth, J.A., Czeplak G. On the estimation of atmospheric radiation from surface meteorological data. Solar Energy. 1996. 56 (4). Pp. 349–359.
8. Vall, S., Castell, A. Radiative cooling as low-grade energy source: A literature review. Renewable and Sustainable Energy Reviews. 2017. 77 (August 2016). Pp. 803–820. DOI: 10.1016/j.rser.2017.04.010
9. Parker, J. The Leeds urban heat island and its implications for energy use and thermal comfort. Energy and Buildings. 2021. 235(September 2013). DOI: 10.1016/j.enbuild.2020.110636
10. Evangelisti, L., Guattari, C., Gori, P., Bianchi, F. Heat transfer study of external convective and radiative coefficients for building applications. Energy and Buildings. 2017. 151. Pp. 429–438. DOI: 10.1016/j.enbuild.2017.07.004
11. Liao, W., Hong, T., Heo, Y. The effect of spatial heterogeneity in urban morphology on surface urban heat islands. Energy and Buildings. 2021. 244. DOI: 10.1016/j.enbuild.2021.111027
12. Korniyenko, S.V., Astafurova, T.N., Kozlova, O.P. Energy Efficient Major Overhaul in Residential Buildings of the First Mass Series. IOP Conference Series: Materials Science and Engineering. 2020. 753 (4). DOI: 10.1088/1757-899X/753/4/042039
13. Millers, R., Korjakins, A., Lešinskis, A., Borodinecs, A. Cooling panel with integrated PCM layer: A verified simulation study. Energies. 2020. 13 (21). DOI: 10.3390/en13215715
14. Kalamees, T., Lupíšek, A., Sojková, K., Mørck, O.C., Borodinecs, A., Almeida, M., Rovers, R., Op'Tveld, P., Kuusk, K., Silva, S. What kind of heat loss requirements NZEB and deep renovation sets for building envelope? CESB 2016 – Central Europe Towards Sustainable Building 2016: Innovations for Sustainable Future. 2016. (October 2019). Pp. 137–144.
15. Baranova, D., Sovetnikov, D., Borodinecs, A. The extensive analysis of building energy performance across the Baltic Sea region. Science and Technology for the Built Environment. 2018. 24 (9). Pp. 982–993. DOI: 10.1080/23744731.2018.1465753.
16. Gaujena, B., Borodinecs, A., Zemitis, J., Prozuments, A. Influence of building envelope thermal mass on heating design temperature. IOP Conference Series: Materials Science and Engineering. 2015. 96 (1). DOI: 10.1088/1757-899X/96/1/012031
17. Borodinecs, A., Prozuments, A., Zajacs, A., Zemitis, J. Retrofitting of fire stations in cold climate regions. Magazine of Civil Engineering. 2019. 90 (6). Pp. 85–92. DOI: 10.18720/MCE.90.8
18. Borodinecs, A., Geikins, A., Prozuments, A. Energy consumption and retrofitting potential of Latvian unclassified building. 2020. DOI: 10.1007/978-981-32-9868-2_27.
19. Dimdina, I., Krumins, E., Lesinskis, A. Indoor Air Quality in Multi-Apartment Buildings before and after Renovation. Construction Science. 2015. 16 (1). Pp. 3–10. DOI: 10.1515/cons-2014-0006
20. Korniyenko, S. Complex analysis of energy efficiency in operated high-rise residential building: Case study. E3S Web of Conferences. 2018. 33. DOI: 10.1051/e3sconf/20183302005
21. Vatin, N., Korniyenko, S.V., Gorshkov, A.S., Pestryakov, I.I., Olshevskiy, V. Actual thermophysical characteristics of autoclaved aerated concrete. Magazine of Civil Engineering. 2020. 96 (4). Pp. 129–137. DOI: 10.18720/MCE.96.11
22. Korniyenko, S.V., Vatin, N.I., Gorshkov, A.S. Thermophysical field testing of residential buildings made of autoclaved aerated concrete blocks. Magazine of Civil Engineering. 2016. 64 (4). Pp. 10–25. DOI: 10.5862/MCE.64.2
23. Liepiņš, S., Lešinskis, A., Iljins, U. Low-emission heat insulation for roof constructions. Research for Rural Development. 2012. 2. Pp. 105–108.
24. Observations, U., Nocturnal, T.H.E. Smithsonian Miscellaneous Collections. Nature. 1924. 114 (2855). Pp. 85–85. DOI: 10.1038/114085a0
25. Li, M., Jiang, Y., Coimbra, C.F.M. On the determination of atmospheric longwave irradiance under all-sky conditions. Solar Energy. 2017. 144. Pp. 40–48. DOI: 10.1016/j.solener.2017.01.006
26. Chen, B., Maloney, J., Clark, D., Mei, W.N. Measurement of night sky emissivity in determining radiant cooling from cool storage roofs and roof ponds. Proceedings of the National Passive Solar Conference. 1995. 20 (1). Pp. 1–6.
27. Evangelisti, L., Guattari, C., Asdrubali, F. On the sky temperature models and their influence on buildings energy performance: A critical review. Energy and Buildings. 2019. 183. Pp. 607–625. DOI: 10.1016/j.enbuild.2018.11.037
28. Levinson, R., Akbari, H., Berdahl, P. Measuring solar reflectance-Part I: Defining a metric that accurately predicts solar heat gain. Solar Energy. 2010. 84 (9). Pp. 1717–1744. DOI: 10.1016/j.solener.2010.04.018
29. Andreas, E.L., Ackley, S.F. On the differences in ablation seasons of Arctic and Antarctic sea ice. 1982. 0469 (December). DOI: 10.1175/1520-0469(1982)039<0440
30. Flerchinger, G.N., Xaio, W., Marks, D., Sauer, T.J., Yu, Q. Comparison of algorithms for incoming atmospheric long-wave radiation. Water Resources Research. 2009. 45 (3). DOI: 10.1029/2008WR007394

31. Chen, J., Lu, L. Development of radiative cooling and its integration with buildings: A comprehensive review. Solar Energy. 2020. 212 (October). Pp. 125–151. DOI: 10.1016/j.solener.2020.10.013
32. Maghrabi, A., Clay, R. Nocturnal infrared clear sky temperatures correlated with screen temperatures and GPS-derived PWV in southern Australia. Energy Conversion and Management. 2011. 52 (8–9). Pp. 2925–2936. DOI: 10.1016/j.enconman.2011.02.027
33. Environments, U. Healthy, Intelligent and Resilient Buildings and Urban Environments. 7th International Buildings Physics Conference, IBPC2018. 2018. (September 2018). Pp. 6.
34. Incropera, F.P., DeWitt, D.P. Fundamentals of Heat and Mass Transfer. 1996. (December 2018). Pp. 890. DOI: 10.1016/j.applthermaleng.2011.03.022
35. Chen, D., Chen, H.W. Using the Köppen classification to quantify climate variation and change: An example for 1901-2010. Environmental Development. 2013. 6 (1). Pp. 69–79. DOI: 10.1016/j.envdev.2013.03.007
36. Porcaro, M., Ruiz de Adana, M., Comino, F., Peña, A., Martín-Consuegra, E., Vanwalleghem, T. Long term experimental analysis of thermal performance of extensive green roofs with different substrates in Mediterranean climate. Energy and Buildings. 2019. 197. Pp. 18–33. DOI: 10.1016/j.enbuild.2019.05.041

Information about author:

Sergey Korniyenko,
Doctor in Technical Science
ORCID: https://orcid.org/0000-0002-5156-7352
E-mail: svkorn2009@yandex.ru

Received 02.06.2021. Approved after reviewing 17.11.2021. Accepted 29.11.2021.